Modern clinical Mtb strains leverage the type I IFN pathway for a pro-inflammatory response in the host

Deepthi Shankaran[1,2#], Prabhakar A[1, 2#], Sheetal Gandotra[1,2], Vivek Rao[1,2]*

1-CSIR- Institute of genomics and Integrative Biology, Mathura Road, New Delhi-110025 India.

2- Academy of Scientific and Innovative Research (AcSIR), ACSIR- Human Resource Development Centre, (CSIR-HRDC) Campus, Uttar Pradesh- 201 002 India

#- Equal contribution

*Corresponding author: Tel: +91 11 29879229, E-mail: vivek.rao@igib.res.in

Running title: Type I IFN induction is Mtb strain dependent

Key words: Mycobacterium tuberculosis/ clinical lineages/ Type I IFN/ macrophage/ Mitochondria

---

ABSTRACT:

Host phagocytes are adept at responding to infections by innate immune mechanisms and metabolic alterations designed to restrict the invading pathogen. However, this very plasticity of the response provides an ideal platform for pathogen mediated manipulation. Clinical lineages of *Mycobacterium tuberculosis* have evolved distinct and numerous ways of achieving optimal infection. We demonstrate an early, active and prominent induction of the macrophage type I IFN response by the modern lineages (L3 and L4) in contrast to the protracted and diminished capacity of the ancient Mtb lineage L1. We also establish a unique link between this augmented IFN response and increased expression of the CH25H, a pro-inflammatory signaling molecule that regulates the early and enhanced pro-inflammatory response (IL6) in macrophages infected with modern Mtb strains. We reveal a strong correlation between the localization of modern Mtb to acidified phagosomes and the ability to induce type I IFN in macrophages highlighting yet another unique ability of Mtb to manipulate host cell physiology to foster a pro-inflammatory response from host phagocytes.

Abbreviations: IFN- Interferon, STING- Stimulator of IFN genes, TRIF- T IR domain containing adaptor inducing IFN, cGAS- cyclic GMP- AMP- synthase, BAF A- bafilomycin A, MDM- monocyte derived macrophages, Mtb- *Mycobacterium tuberculosis*, BCG- *Bacille Calmette Guerin*, CH25H- cholesterol 25 hydroxylase, lyso^{+}- lysotracker positive.

Introduction:

A long-standing association with the human population has been critical to the development of specific immune modulatory mechanisms by *Mycobacterium tuberculosis* (Mtb) for efficient survival within the host. Following the initial contact of Mtb with macrophages, the type I IFN response pathway is strongly activated [1, 2, 3]. A clear dependence on both the host and pathogen associated factors is observed for Mtb mediated induction of IFN signaling in macrophages [4, 5, 6]. While active damage of host mitochondria by ROS and subsequent discharge of DNA into the cytosol to facilitate the cGAS-STING/ NOD2- RIP signaling pathways is crucial, Mtb ESX-1 mediated phagosomal escape, cytosolic leakage of endosomal constituents and mycobacterial cyclic di-nucleotides also play dominant roles in the induction of the type I IFN response [2, 7]. Given a central role for bacteria associated factors, it is not surprising that significant variations in inflammatory response induction and virulence are now being appreciated amongst the different Mtb lineages prevalent in the human population [8, 9, 10]. However, the exact molecular mechanisms of these differences are not yet completely understood.

In this study, we demonstrate that clinical strains belonging to the modern lineages (L3, L4 and L2) can actively induce the type I IFN response in macrophages contrasting with the attenuated response to L1 Mtb and BCG strains despite the presence of an active ligand. This response is dependent on lysosomal association of strains. We observe a linear correlation between the higher IFN inducing Mtb- L3 trafficking to these lyso^{+} compartments early and at higher frequencies than the less proficient-L1 strain. We also demonstrate a clear protracted pro- inflammatory response associated with infection of macrophages by the L1 Mtb strains.

Recent evidence connects type I IFN induced cholesterol 25-Hydroxylase (CH25H) with the expression of pro-inflammatory cytokines like IL6 in response to TLR stimulation/ viral infection of macrophages [11, 12, 13 14, 15]. We conclusively show that the modern Mtb strain L3 can actively engage the type I IFN signaling machinery and activate the expression of CH25H in order to facilitate the early and higher expression of IL6 from host cells. This study provides evidence for a novel mechanism of the plasticity of modern Mtb by coupling type I IFN with macrophage pro-inflammatory response. Understanding the physiological consequence of this phenomenon would provide crucial insights into the successful adaptation of modern Mtb to the host environment.

Results:

Mtb lineages induce differential type I IFN response in macrophages.

Macrophages respond to mycobacterial infection by elaborating an array of signaling cascades and effector functions. The type I IFN response has generated interest as a pro- pathogenic response induced by Mtb strains in macrophages [16, 17, 18, 19]. THP1 macrophages infected with Mtb Erdman responded with a prominent IFNβ gene induction by 6h that was sustained even by 24h of infection that translated as a time dependent expression of the several ISGs (IFN stimulated genes) and effector genes (Fig.1A,B). This response is well recapitulated in an IFN reporter cell line- THP1 dual that also portrays a dose and temporal response to Mtb infection. While the levels of secreted luciferase were not detectable until 12h of infection, we observed 5-10 folds higher activity in Mtb infected macrophages by 24h and 48h (Fig.1C). We used this reporter line to assess the lineage specific activation profile amongst clinical Mtb strains. Macrophages infected with the modern Mtb lineages (III-N4, N24; II- HN878, IV-H_{37}Rv, Erdman) displayed 8-20 folds higher luminescence activity than the uninfected cells at 24h of infection, contrasting with the lower activity (1.5-2 folds) in macrophages infected with the ancient lineage I (N72, N73) Mtb strains (Fig.1D). While neither of the *M. bovis* BCG strains induced any response, both H_{37}Rv and H_{37}Ra (Fig. S1A) induced the IRF promoter to comparable levels. This higher IRF activation potential of L3 Mtb was maintained across different infective doses

(Fig. 1E) wherein, L3 Mtb strains (N4 and N24) could activate this response even at a low MOI of 1 (4.6 folds) by 24h of infection higher than the average levels of ~3 folds IFN response induction by 10 fold higher doses of L1 Mtb strains (N72 and N73 at MOI-10). This trend was maintained even at the 48h time point of infection arguing for the inherent lower IFN activating potential of the L1 Mtb lineage.

Gene expression profiles further validated the temporal and differential IFNβ expression profiles of Mtb infected macrophages; as observed in Fig. 1F, the L3 Mtb strain-N24 beginning to induce IFNβ mRNA as early as 1h with a gradual increase (~30 folds by 12h of infection) that was sustained even by 24h of infection (~16folds). Contrastingly, the L1 (N73) strain never supported high levels of IFN expression at any time in the study. Moreover, IFNβ transcript was detected on by 6-12h of infection at ~7 fold lower levels even by 24h of N24 infection. Primary human MDMs from healthy individuals also showed 4-8 fold higher levels of expression of type I IFN pathway genes (IFNβ, IFIT2, IP10) in response to infection with N24 in comparison to infection with N73 at 6h (Fig. 1G). Even in the mouse macrophage line RAW264.7 cells, L1 Mb exhibited a refractory type I IFN inducing behavior (Fig. 1H). Taken together, these data suggest that active IFN induction is Mtb lineage specific phenomenon conserved across human and mouse macrophages.

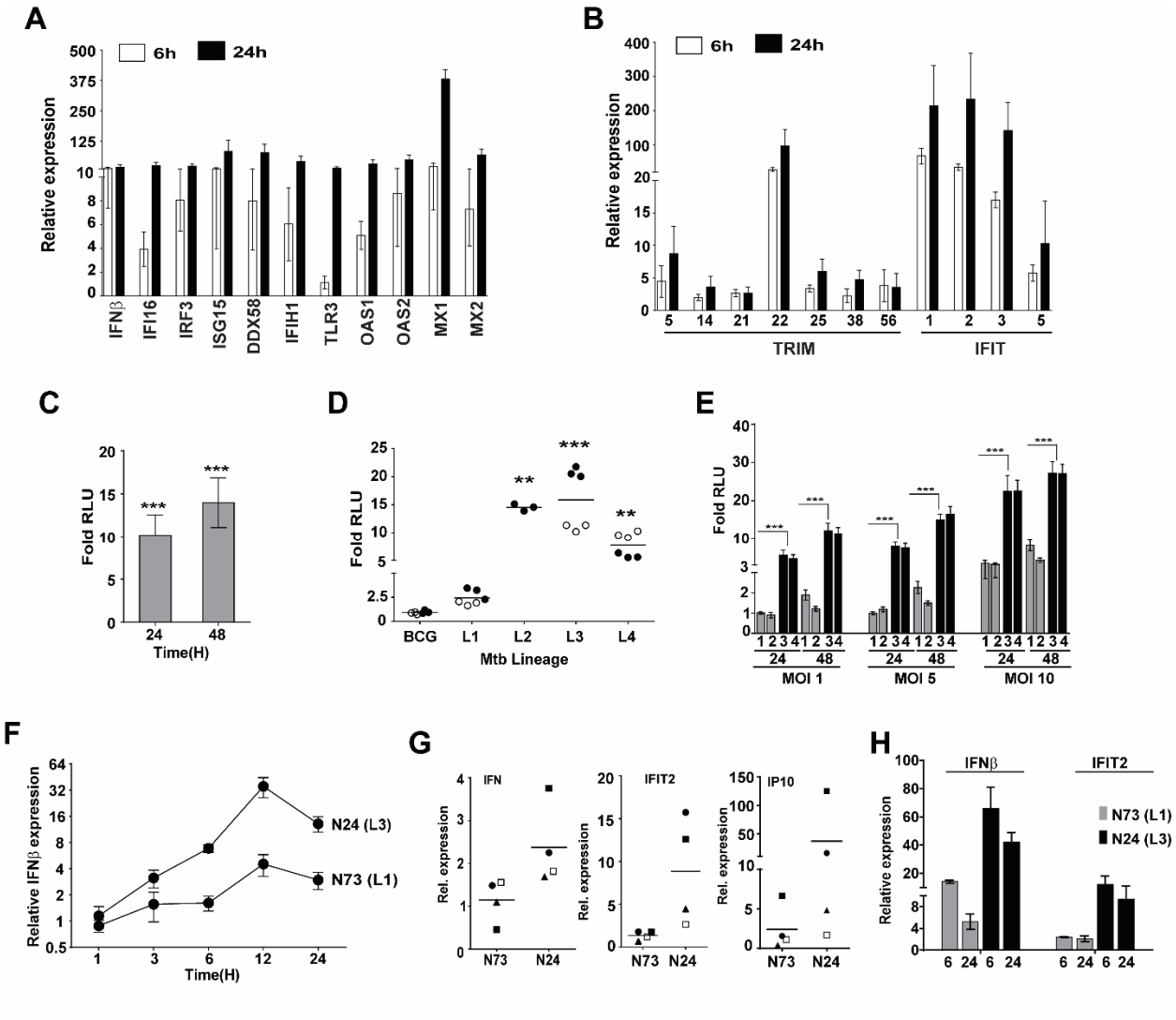

Fig.1

Fig.1: Modern lineages have evolved to induce a significantly higher type I IFN response

A, B) Expression of IFNβ and ISGs in THP1 macrophages infected with Mtb Erdman at a MOI of 5. At 6h and 24h post infection, expression of IFNβ/ ISGs and GAPDH was analyzed by qPCR. Values represent average fold expression gene ± SD in infected and control samples from triplicate wells of a representative experiment.

C) Relative luciferase activity in THP1 macrophages, left uninfected or infected with Mtb Erdman at a MOI of 5. At the indicated time points, culture supernatants were harvested and tested for luciferase expression. Values represent average ratios of RLU in infected and control samples (± SEM) of N=3.

D) Relative luciferase activity in THP1 dual macrophages left uninfected or infected with Mtb strains belonging to different lineages (I-IV) at a MOI of 5. The 2 independent isolates of each lineage used for infection is represented as open and closed circles. After 24h of infection, culture supernatants were

harvested and tested for luciferase expression. Values represent average ratios of RLU for the lineage from triplicate wells of a representative experiment of N=2.

E) Relative luciferase activity in THP1 dual macrophages left uninfected or infected for 24h with Mtb L1 (grey bars; 1-N72, 2-N73) and L3 (black bars; 3- N4, 4-N24) at different MOIs indicated below. At the indicated time points, culture supernatants were harvested and tested for luciferase expression. Values represent average ratios ± SE of RLU in infected and control samples from triplicate wells of two independent experiments (N=2).

F) Relative expression of IFNβ mRNA in THP1 dual macrophages infected with N24 (L3) or N73 (L1) at a MOI-5. At different time intervals post infection, expression of IFNβ and GAPDH was analysed by qPCR. Values represent average fold expression of IFNβ ± SE in infected and control samples from triplicate wells of three independent experiments (N=3).

G) Relative expression of IFNβ, IFIT2 and IP10 mRNA in primary MDMs from four separate individuals (symbols) infected with N24 or N73 for 6h at a MOI-5. The expression of type I IFN genes and GAPDH was analyzed by qPCR. Median values are indicated by a line.

H) Relative expression of IFNβ, and IFIT2 mRNA in RAW264.7 macrophages infected with N24 (black bars) or N73 (grey bars) for 6h and 24h at MOI-5. The expression of type I IFN genes and GAPDH was analyzed by qPCR. Relative expression values ± SD are represented.

L1 Mtb are delayed in inducing type I IFN response in macrophages despite the presence of an active ligand.

Given the deferred IFN response by L1 Mtb, it was logical to assume either a lack of appropriate quantities of the interacting ligand with the IFN signaling cascade or suppression of the IFN response by this Mtb strain. Macrophages infected with non-viable Mtb failed to initiate this response proving that the IFN response was actively induced by Mtb (Fig. 2A). Having ascertained that the response was an active process, we next checked if one Mtb strain could actively modulate the response of the other. To test this, we employed a co-infection assay wherein N24 and N73 were used to infect macrophages either alone or together in different ratios to evaluate the competitive IFN inducing capacity of strains (Fig. 2B). At all doses tested, N24 induced significantly higher response than N73. In macrophages infected with a mixture of the two strains, inclusion of 20% N24 Mtb (N73:N24 :: 4:1) was sufficient to enhance the IFN response to levels comparable to N24 alone at MOI-1; this gradually increased with the proportion of N24 in the inoculum-50% (N73:N24::2.5:2.5). Most importantly, the presence of

N73 at high concentrations (4x) could not diminish the response induced by N24 in the co-infection model (N73:N24 :: 4:1). This was also evident at the higher MOI of infection of 10, wherein presence of 50% of N73 did not dampen the N24 mediated IFN response.

Further validation was achieved in a trans- activation/ suppression assay using poly IC (pIC) individually or in combination with either of the lineages. Poly IC alone induced a dose dependent type I response in THP1 dual macrophages (Fig.2C). The response to poly IC, however was clearly augmented in conditions of co-stimulation with either N24 or N73. Overall the increment in response of N24 was marginal reaching only 2.3 folds higher with 10µg/ml of pIC, in contrast, response of N73 in combination with as low as 1µg/ml pIC was higher by 2.1 folds; with 10 µg/ml pIC, this increased by 10.5 folds proving that N73 strain did not suppress the IFN response in macrophages.

Given the importance of a nucleic acid signaling mediated expression of type I IFN in macrophages, we tested Mtb extracts for their ability to prime the IFN response in THP1 cells (Fig. 2D,E). Crude lysates of Erdman induced a temporal IFN response, increasing from ~10 folds at 3h to ~75 folds by 6h and then declining to ~10fold expression by 24h of stimulation with different doses (Fig. 2D). In fact, as low as 1.6 ng of the extract was sufficient to induce this response (~10folds) by 6h (Fig. S2-A). While extracts subjected to enzymatic digestion with DNase completely lost their IFN inducing capability (Fig. 2E), treatment with protease, RNase A or heat inactivation did not impede the IFN inducing capacity of the extracts (Fig. S2-B). In fact, as low as 125 ng of genomic DNA from Mtb was sufficient to induce the IFN response in macrophages; again pretreatment with DNase abolished this response (Fig. 2E). It was logical to assume with the lower response of L1 Mtb or BCG that the active ligand inducing the Mtb dependent type I IFN response would either be in lower concentrations or ineffective in IFN induction in these strains. Surprisingly, both the extracts and genomic DNA from N73 as well as BCG were similar to Erdman and N24 in their IFN inducing capacities (Fig. 2F), implying that

while an active ligand (DNA) was available in these strains, it remained inaccessible to the IFN signaling machinery of macrophages.

Further confirmation of the importance of nucleic acid signaling was achieved in macrophages impaired in the signaling receptor/ adaptor (cGAS/ STING). As observed for THP1 cells, Wt RAW-luc (ISG) cells also portrayed a differential type I IFN response with the different Mtb lineages -both the L1 strains (N72 and N73) failed to enhance the type I response significantly in contrast to the 5-10 folds upregulation by the L3 Mtb strains (Fig. 2G). However, cGAS or STING deficient macrophages failed to elaborate type I IFN even following infection with L3 Mtb implicating a dominant role of this signaling axis in this response against mycobacteria. Loss of the RNA signaling receptor TRIF also resulted in a significant (~60% decrease) in Mtb induced IFN response in macrophages arguing for an essential role for nucleic acid signaling mechanisms in type I IFN induction by Mtb. However, absence of RIG 1, MDA5 or MAVS did not critically alter this response (Fig. S2-C). Surprisingly, even BCG which lacks an inherent IFN inducing capacity, was capable of inducing this response following delivery of BCG along with the transfection agent- lipofectamine- LTX into macrophages. This LTX assisted delivery of the bacteria supported ~3-6 fold higher IFN than BCG infection alone at a MOI of 5 by 24h of infection (Fig. 2H).

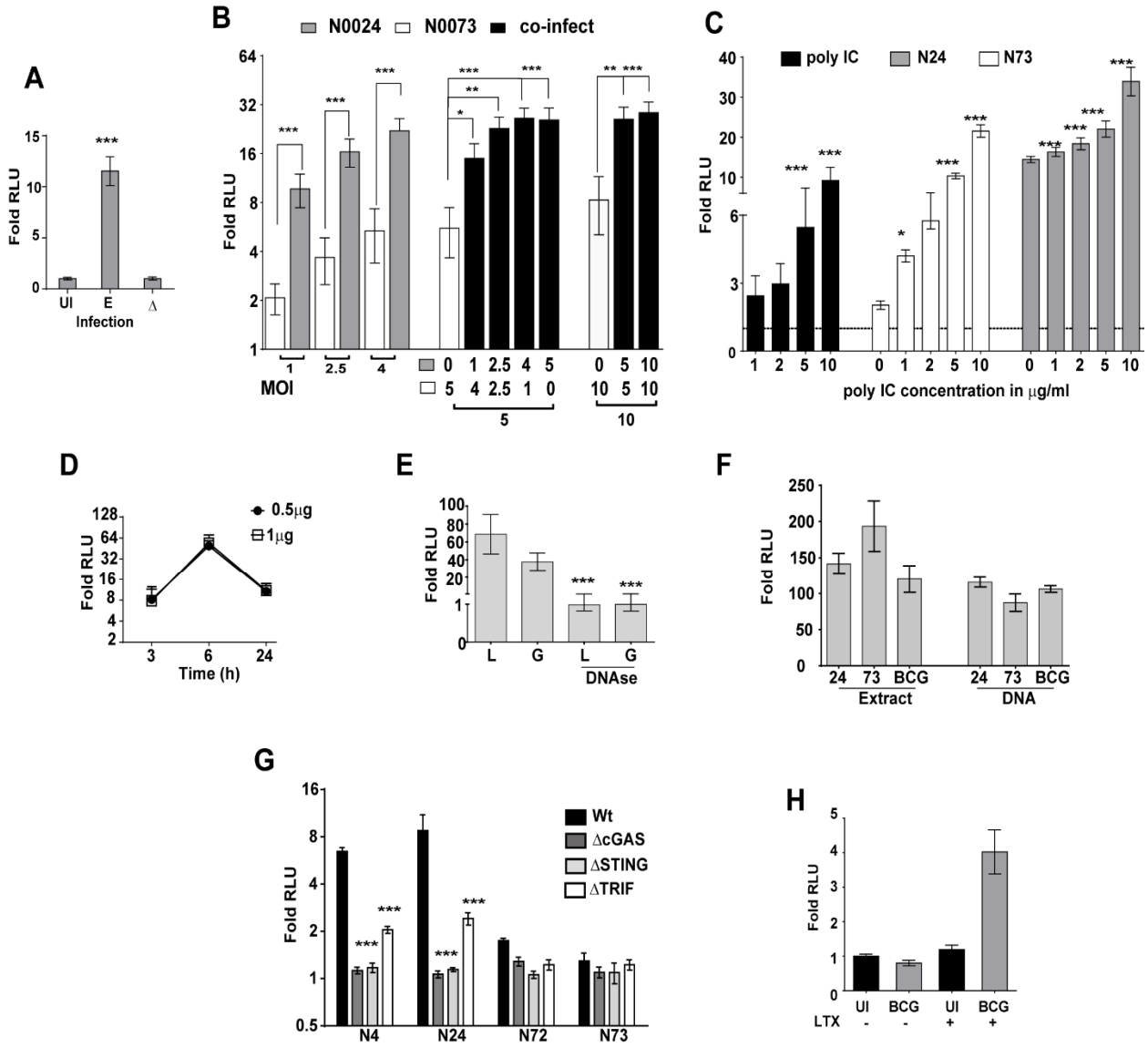

Fig. 2

Fig.2: Strains with suppressed type I IFN response are well equipped with the active IFN inducing ligand.

A) Relative luciferase activity in THP1 dual macrophages left uninfected (UI) or infected with live or heat killed (Δ) Mtb Erdman at a MOI of 5 for 24h. Values represent average ratios of infected and control RLU ± SD from triplicate wells of an independent experiment.

B) Relative luciferase activity in THP1 dual macrophages left uninfected or infected with N24 (grey bars), N73 (white bars) or in different combinations (black bars) as indicated. At 24h *p.i.*, culture supernatants were harvested and tested for luciferase expression. Values represent average ratios ± SE of RLU in infected and control samples from triplicate wells of three independent experiments (N=3).

C) Relative luciferase activity in THP1 dual macrophages left uninfected or stimulated with different concentrations of poly IC (black bars) alone or in combination with N24 (grey bars)/ N73 (white bars) as indicated. Values represent average ratios ± SE of RLU in infected and control culture supernatants from triplicate wells of three independent experiments (N=3). Value signifying the unchanged expression (X=1) is indicated by a line.

D) Relative luciferase activity in THP1 dual macrophages post transfection with two concentrations of crude Erdman lysates at 3, 6 and 24h.

E) Response of macrophages to lysate (L) or genomic DNA (G) alone or treated with DNAse.

F) IRF promoter response of THP1 dual cells treated with crude lysates/ DNA of Mtb N24, N73 or BCG at 6h. Values represent average ratios ± SD of RLU in infected and control samples from triplicate wells of two independent experiments.

G) Relative luciferase activity in wild type (Wt, ISG) or gene deficient RAW264.7 macrophages uninfected or infected with Mtb strains belonging to L3 / L1 lineages at a MOI of 5 for 24h. Values represent average ratios ± SE of RLU in infected and control culture supernatants from triplicate wells of three independent experiments (N=3).

H) Relative luciferase activity in THP1 macrophages following infection with BCG or BCG and lipofectamine (LTX+) at a MOI of 5 for 24h. Values represent average ratios ± SE of RLU in infected and control samples from triplicate wells of N=2.

IFN inducing capability correlates with induction of a pro-inflammatory response via expression of CH25H in macrophages.

To understand if the L1 Mtb strains were also affected in their overall ability to activate macrophages, we tested gene expression and cytokine profiles of RAW264.7 macrophages infected with L1 and L3 Mtb. Both TNF and IL6 patterns were strikingly similar to type I IFN, with lower levels in the case of L1 than the L3 infected RAW264.7 macrophages after 24 hours (Fig. 3A). While IL6 was more or less not induced by the L1 Mtb strains, there was a 4-5-fold higher TNF in the N24 infected macrophages as compared to the N73 infected cells. The levels of IL1β, however, were similar in the two cells. This attenuated TNF and IL6 inducing pattern was also observed following infection of primary bone marrow-derived macrophages from C57BL/6 mice (Fig. 3B) and human monocyte derived macrophages wherein a significantly protracted response was observed with L1 Mtb infection (Fig. S3). In fact, L1 Mtb induced significantly lower levels of IL6 in a temporal manner from macrophages (Fig. 3C). IL6 levels gradually

increased in response to L3 infection until 48h and was maintained thereafter in contrast to the insignificant levels of IL6 in macrophages supernatants even as late as 48-72h following L1 Mtb infection.

The lower IFN and IL6 secretion associated with L1 Mtb suggested a common mechanism of regulation in the macrophage response pathway by this mycobacterial strain. Initially, we analyzed if the decreased IL6 protein levels in the L1 infected macrophages was due to an alteration in gene expression levels by qPCR. Again, the expression of IL6 in the L1 infected macrophages was more delayed than in L3 infected BMDMs. Macrophages infected with N24 secreted ~30-fold higher IL6 levels than N73 by 6h of infection (Fig. 3D). At the later time point of 24h, despite a dip the IL6 levels in N24 infected macrophages were still significantly higher than in N73 infected cells suggestive of a protracted and lower response initiation by the L1 Mtb strains.

The complete dependence of IL6 expression on type I IFN induction was evident in STING deficient macrophages (ΔS). Levels of IL6 were significantly decreased (5-6 fold) in response to Mtb infection in these deficient macrophages at 6h and 24h of infection, completely nullifying the difference of IL6 expression between the N24 and N73 Mtb strains observed in the Wt RAW macrophages (Fig. 3E). Clearly, N73 Mtb, that failed to induce significant IL6 expression, was not affected by the presence or absence of STING in the macrophages. More importantly, STING dependence was only observed for IL6 as loss of STING did not significantly affect the TNF inducing capacity of Mtb in macrophages.

More recently, a positive regulatory circuit for IL6 through the cGAS-STING dependent IFN response mediated via the pro-inflammatory CH25H gene expression has been identified [15]. Cholesterol metabolites, specifically, oxysterols like 25 hydroxy-cholesterol have been recognized as potent regulators of the pro-inflammatory response of macrophages [13]. As a validation of this regulatory circuit, we compared expression patterns of genes in the cholesterol biosynthetic pathway of BMDM infected with L3 and L1 Mtb (Fig. S4). Overall, a time dependent

differential expression of these genes involved in the cholesterol flux of host cells was evident by qPCR, the expression patterns in the two sets of macrophages were distinct. Most of the genes involved in the cholesterol biosynthetic pathway either up-regulated or similar in L1 infected macrophages after 24h of infection. In contrast, these genes were inhibited in response to infection with L3 Mtb. Surprisingly, in contrast with the overall pathway, expression of CH25H was significantly upregulated in the L3 infected macrophages (60-70 fold higher than the uninfected control) as opposed to the much lower expression of this gene (3-4 folds) in the L1 infected macrophages, by 6h of infection (Fig. 3F). This difference was however lower later at 24h, wherein a sharp decline in L3 (23 folds) and an increase in L1 infected macrophages (10-12 folds) was observed. Expression of most of the cholesterol transport pathway (Insig1, SREBP1, StarD4, SCD1) was higher in the L1 infected macrophages (data not shown).

To test if the higher IFN induced by L3 Mtb contributed to the early increased CH25H, we compared expression in ΔSTING deficient RAW macrophages (Fig. 3G). The complete loss of L3 induced CH25H expression in the mutant cell lines validated the regulatory role of type I IFN in host oxysterol expression.

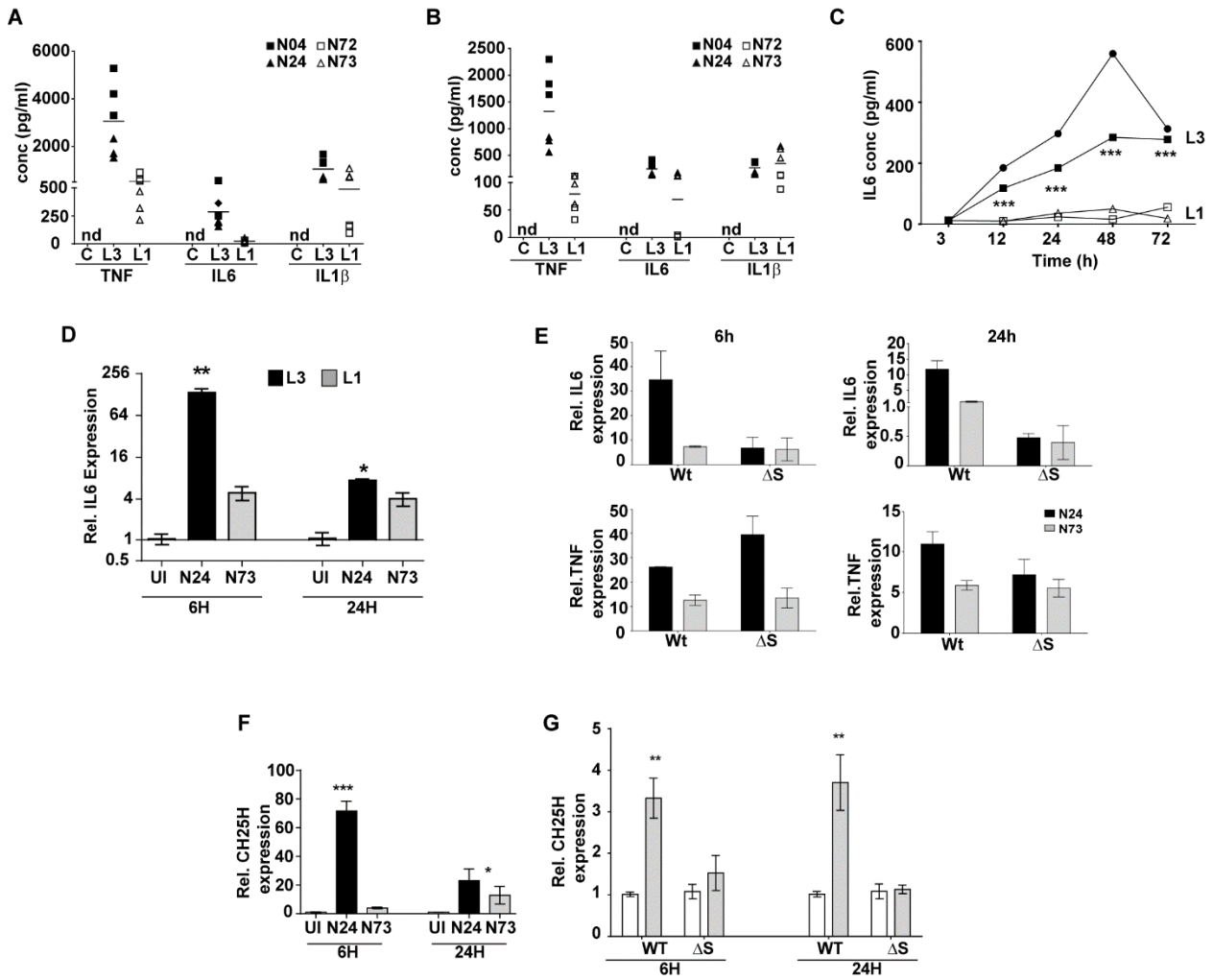

Fig. 3

Fig.3: IL6 response in Mtb infected macrophages primarily depends on type I IFN mediated CH25H expression.

A. TNF, IL6 and IL1β secretion from RAW264.7 macrophages B) from BMDMs of C57BL/6 mice following infection with two L3 or L1 Mtb strains. Values represent IL6 concentration average ratios in pg/ml ± SE at 24h *p.i* in the culture triplicate wells of two independent experiments (N=2).

C) Time kinetics of IL6 secretion from BMDMs of C57BL/6 mice following infection with two L3 or L1Mtb strains. Values represent IL6 concentration average ratios in pg/ml ± SE at different time intervals post infection in the culture triplicate wells of two independent experiments (N=2).

D) IL6 gene expression profiles in BMDM from C57BL/6 mice following infection with N24 (L3) or N73 (L1) Mtb strains. The average relative IL6 values ± SE (with respect to GAPDH) at 6h and 24h post infection in triplicate wells of two independent experiments (N=2) is shown.

E) IL6 and TNF expression from RAW-ISG and ΔSTING macrophages following infection with N24 or N73 strains at 6h and 24h *p.i.* at MOI-5. The relative expression with respect to GAPDH ± SD from triplicate wells of a representative experiments is represented.

F) Expression of CH25H in primary bone marrow derived macrophages following infection with N24 or N73 strains at 6h and 24h *p.i.* at MOI-5. The relative expression with respect to GAPDH ± SD from triplicate wells of a representative experiments is represented.

G) Expression of CH25H in RAW-ISG and ΔSTING macrophages upon mycobacterial infection at 6h and 24h *p.i.* at MOI-5. The relative expression with respect to GAPDH ± SE from three independent experiments (N=3) is represented.

Early localization to lysosomes is important for Mtb induced type I IFN induction

The early induction of type I IFN in L3 infected macrophages (1-3h of infection) advocated for molecular events that ensue immediately after infection as causative. Further, analysis of THP1 macrophages by TEM revealed partitioning of N24 and N73 in distinct intracellular compartments. While, N24 localized to compact double membranous vesicles at 24h in contrast, most of the Mtb N73 cells localized to a loose vesicular structure with membranes with intracellular particles (Fig. 4A). A similar association with compact double membranous vesicles was also reflected in the case of Mtb Erdman, (Fig. S5) hinting at an important role of intracellular vesicular transport. To verify this, we followed the intracellular partitioning of Mtb strains in macrophages over different durations of infection. N24 localized to lysotracker positive (lyso+) vesicles as early as 6h at greater numbers than N73 Mtb (Fig. 4B). Even at 24h, we observed a significantly (~2.5-3) fold higher co-localization of N24 Mtb in lyso+ compartments, in comparison to N73 (Fig. 4C).

The differential localization to lyso+ vesicles between N24 and N73 was not restricted to THP1 macrophages; infection of RAW264.7 also partitioned significantly higher numbers of N24 Mtb in lyso+ vesicles early and over long periods of infection (Fig. 4D). While there was a gradual decrease in N24 in lyso+ positive vesicles with time of infection, the levels of N73 were maintained yet significantly lower throughout the experiment duration. Interestingly, the differential localization arose as early as 1h of infection with Mtb N24 localizing at high numbers to phago-lysosomes than N73. While >50% of N24 were associated with lyso+ vesicles, N73 showed a bimodal distribution with a significant fraction of cells with less co-localization and a

smaller fraction with higher localization. Nearly 2-fold higher numbers of N24 in lysotracker positive vesicles were observed at 3 and 24h *p.i.* (Fig. 4E).

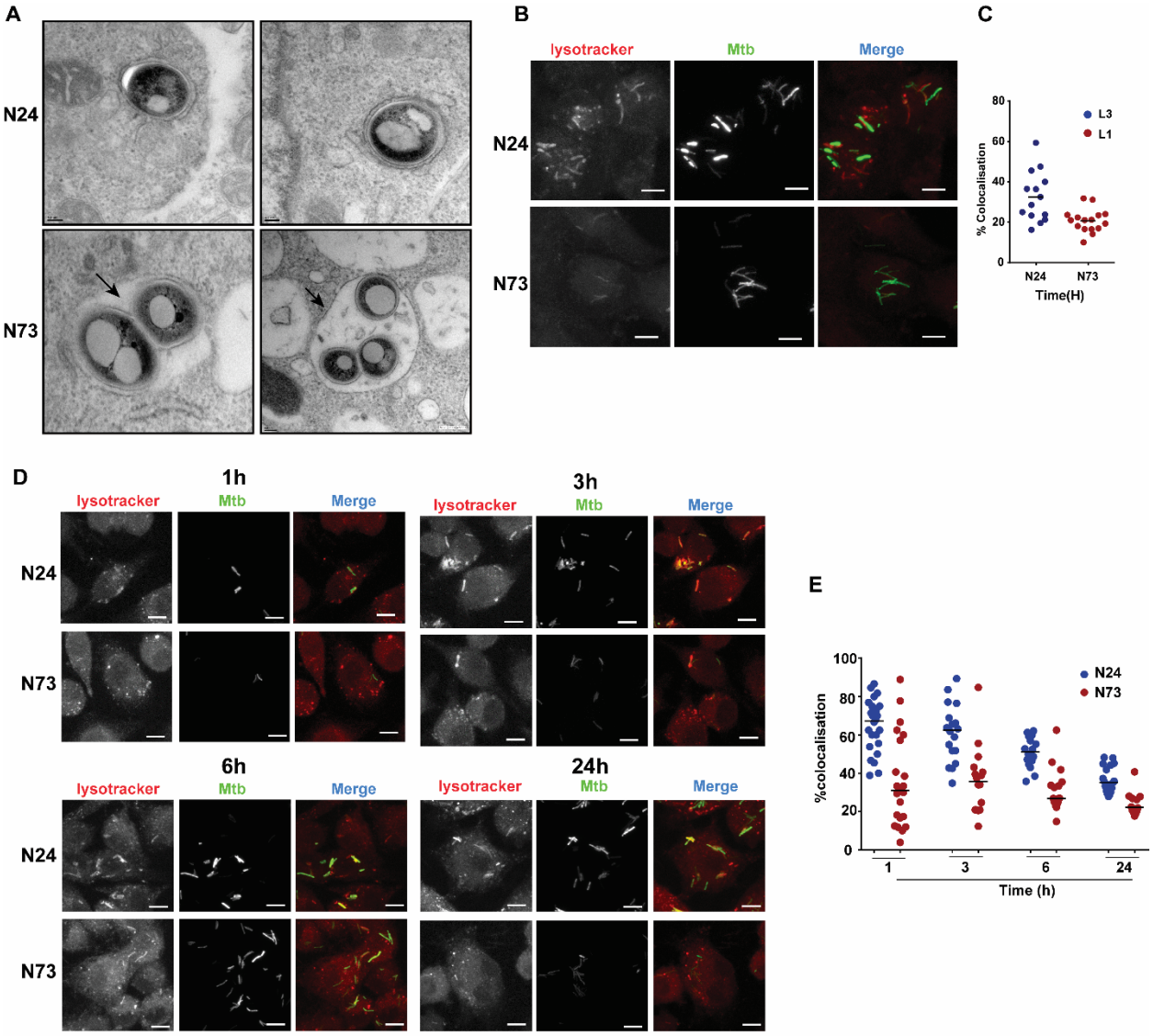

Fig. 4

Fig.4: Early and sustained localization of the high IFN inducing Mtb strains with acidified phagosomes.

A) Representative TEM images (2) of Mtb N24 and N73 in THP1 macrophages at 24h post infection. While N24 is found in compact vesicles, N73 localizes in loose vesicles with cellular debris (black arrow).

B-E) Localization of Mtb N24 and N73 in acidified vesicles. Representative images of macrophages stained with lysotracker red and infected with GFP expressing N24/ N73 - THP1 (B) at 24h or RAW 264. 7 (D) at 1h, 3h, 6hand 24 h post infection is depicted. The extent of co- localization of Mtb with the lyso+ vesicles in THP1, 24h and RAW264.7 at 1h, 3h, 6h and 24h is shown graphically in panel C

and E, respectively. Each dot represents a field of image from 2 independent experiments (> 100 infected cells).

IFN inducing capacity of Mtb relies on efficient acidification of the phagosome.

Given the surprisingly high numbers of N24 localization to lyso^{+} compartments, and comparable intracellular growth rates of N24 and N73, it was reasonable to assume an enhanced propensity of N24 to be better equipped for survival in this subcellular niche as well as induce significantly higher IFN from macrophages. The ability of Mtb to counter phagosomal-lysosomal fusion and acidification events is well recognized [20, 21]. To understand if phagosomal acidification was important for IFN induction, we treated macrophages with an established phagocytosis activation signal (LPS+ IFNγ) or phagosomal acidification blockers- bafilomycin A and chloroquine prior to infection with Mtb. Activation of macrophages with IFNγ and LPS enhanced the presence of bacteria in lyso^{+} vesicles of N24 now found in the lyso^{+} compartments (Fig. 5A). More importantly, the numbers of lyso+ N73 Mtb increased reaching comparable levels as N24 Mtb by 6h of infection (Fig. 5B). Consequently, the differential IFN inducing capability of the two strains was lost with >10-fold higher induction in the IFNγ+ LPS pretreated macrophages infected with N73 (Fig 5C and inset panel). Addition of IFNγ and LPS also significantly boosted IFN induction even in N24 infected macrophages supporting the importance of phagosomal trafficking and acidification in the type I IFN response. On the contrary, treatment with phagosome acidification blockers like bafilomycin A or chloroquine sufficiently stunted (~5 and 2 folds, respectively) the IFN response of even N24 infected macrophages (Fig. 5D) again emphasizing the role for phagosome acidification in Mtb mediated IFN induction in macrophages.

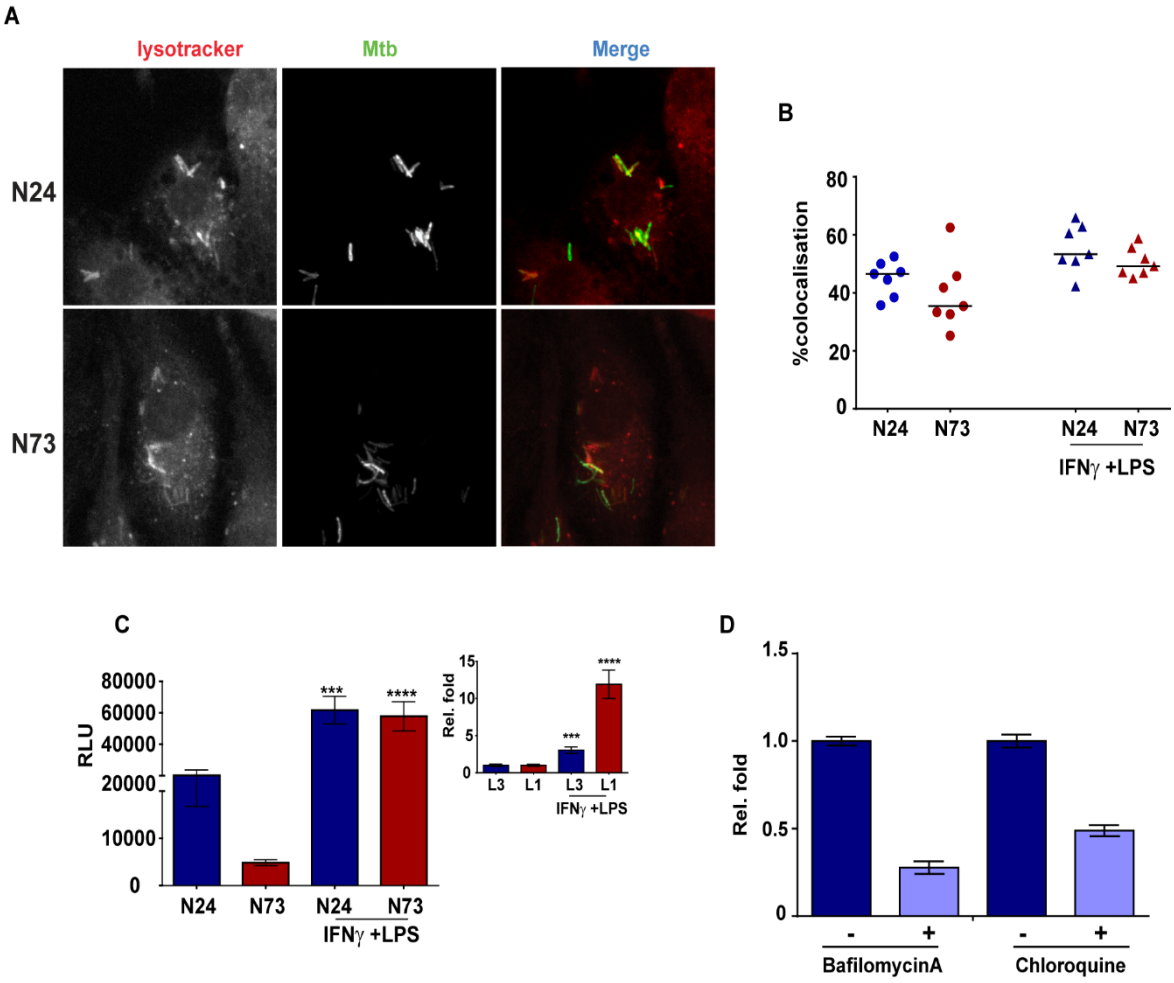

Fig. 5

Fig.5: Phagosomal acidification is crucial for type I IFN induction by Mtb strains.

A) Localization of GFP expressing Mtb N24 and N73 in acidified vesicles (stained with lysotracker red) of RAW 264.7 macrophages treated with murine IFNγ and LPS at 6h post infection.

B) The extent of co- localization of Mtb with the lyso+ vesicles in these macrophages is graphically represented. Each dot represents a field of image from a representative experiment.

C) Relative luciferase activity in RAW264.7 macrophages left untreated or treated with IFNγ and LPS 16h prior to infection with Mtb N24 and N73 at a MOI of 5 for 24h. Values represent average ratios ± SE of RLU in infected and control culture supernatants from triplicate wells of three independent experiments (N=3). The inset represents the fold change in RLU of the treated macrophages with respect to the untreated cells.

D) Relative luciferase activity in RAW264.7 macrophages left untreated or treated with bafilomycin A or chloroquine 1h prior to infection with Mtb N24 and N73 at a MOI of 5 for 24h. Values represent average ratios ± SE of RLU in infected and control culture supernatants from triplicate wells of independent experiments (N=2).

The working model

Clinical Mtb strains differ in their capacities to access the host phago-lysosomal (P-L) pathway; modern lineages traffic via this axis better and localize in lysosomal compartments of host macrophages. In contrast, the older Mtb strains preferentially associate with the early endosomal compartments and traffic less into the P-L pathway. This reduced movement hinders the access of IFN inducing Mtb DNA to the nucleic acid response pathway and significantly lower type I IFN response. The higher activation of type I IFN by the modern strains manifests as a substantial upregulation of CH25H expression and consequent 25-hydroxy cholesterol levels in macrophages that enhances expression of the pro-inflammatory cytokine IL6 in a positive feedback loop.

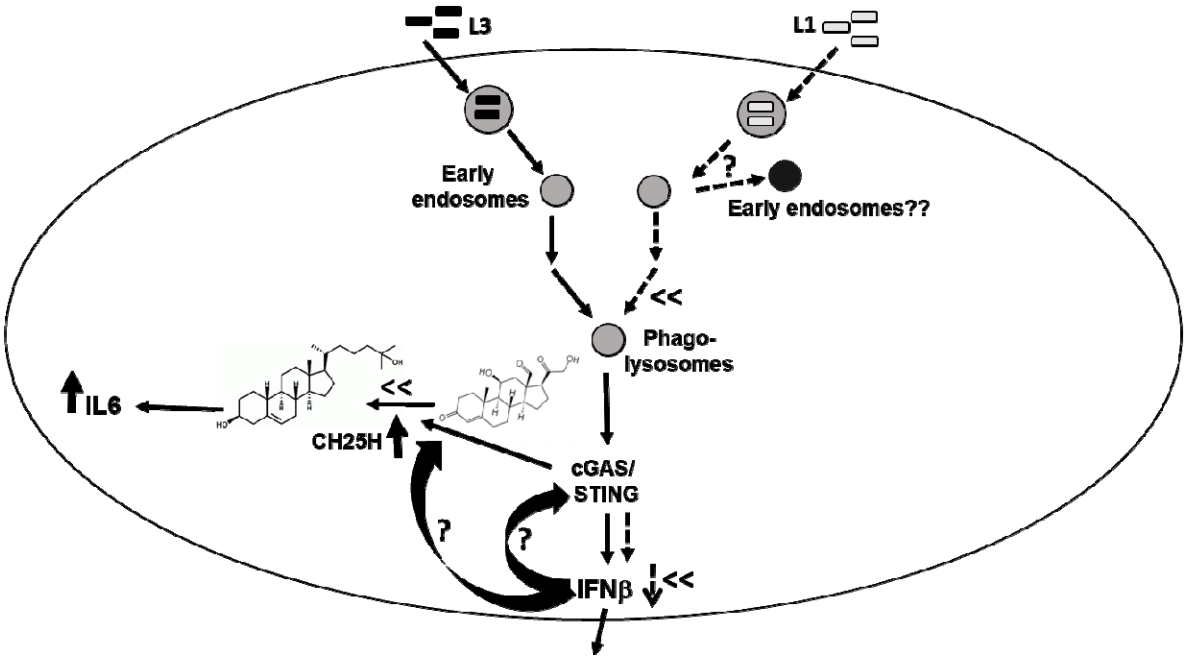

Fig.6: A putative working model of modern Mtb induced IFN and subsequent IL6 expression via the STING-CH25H pathway.

DISCUSSION

The grand success of Mtb as a human pathogen stems from extreme plasticity to suit the host cell niche, modulate the host response and survive multiple intracellular stresses. The

immediate response of host phagocytes upon contact is the activation of inflammatory responses aimed at controlling the growth of the invading pathogen.

While typically the type I IFN response is directed to viral infections, recent studies have highlighted the macrophage expression of type I IFNβ in response to intracellular (pathogenic) and extracellular bacterial (protective) infections [22, 23, 24, 25, 26, 27]. We observed that the modern lineages are more adept at inducing this response in macrophages than the evolutionarily older strains of Mtb. Surprisingly, we did not observe any change in IFN elicitation by $H_{37}Rv$ or its avirulent derivative $H_{37}Ra$. While it is well appreciated that the two strains show differential esx-1 mediated secretory functions, our results do not implicate the esx-1 operon in macrophage type I IFN induction [28]. This is further supported by the comparable expression of ESAT6 in the clinical Mtb lineages (L1 and L3) with significant difference in their IFN inducing capabilities (Fig. S1B). Additionally, contrary to prior reports [4], we did not observe any conclusive evidence for differential mitochondria associated factors in the IFN induction by these strains- 1) comparable changes in mitochondrial ultrastructure by both N73 and N24 infections, 2) similar levels of mtROS at all in infection (Fig. S6A,B).

We observed a linear relationship of Mtb's capacity to stimulate type I IFN with the ability of strains to induce a pro-inflammatory response. Importantly, loss of STING completely reversed Mtb's ability to induce IL6 expression without altering TNF expression levels. The regulatory role for viral infection induced IFN in modulating host oxysterol, specifically CH25H levels, that subsequently controls IL6 gene expression in host cells suggested a similar mechanism for the IFN mediated IL6 expression in the L3 Mtb infected macrophages [15, 29]. Given the lower expression of genes for cholesterol biosynthesis in the late stage of infection with N24 Mtb similar to earlier reports [30], it was surprising that expression levels of CH25H were on the contrary, greatly increased, authenticating the importance of IFN signaling in CH25H expression and insinuated an important role for the host 25- hydroxyl cholesterol in bridging type I IFN and IL6 expression in macrophages. Moreover, the complete loss of CH25H expression in the STING deficient macrophages following N24 infection highlights the novel regulatory loop of

type I IFN- CH25H- IL6 regulation in modern Mtb infections. In contrast, N73 infected macrophages displayed significant increase in expression of biosynthesis but a markedly decreased expression of CH25H in the later stages of infection.

As demonstrated previously, loss of STING/ cGAS completely abrogated Mtb type I IFN response in macrophages implicating cellular DNA signaling as a predominant mechanism of this response. Given the early induction of type I IFN and the absence of this response despite the presence of active ligand, we argued that a novel mechanism that actively concealed the DNA from the cellular nucleic acid signaling mechanism was responsible for the lower IFN induction by the attenuated ancient Mtb strains. Interestingly, loss of TRIF also resulted in absence of IFN response in N24 infected macrophages suggesting a role for RNA signaling in this response. Surprisingly, we did not observe loss of IFN induction by cellular extracts treated with RNAse. Recent reports have identified a TRIF dependent activation of STING in the DNA induced IFN response of macrophages [31]; our results demonstrate a dominant role for this signaling pathway in Mtb mediated type I IFN response. A recent study has demonstrated increase in IFN production by a secondary mechanism of cGAS stabilization mediated by the IFN induced TRIM14 in HSV infected cells [32]. Our results also show temporally enhanced TRIM14 expression (2 and 6 folds in N24 infected cells as compared to 1 and 2 folds in N73 infected macrophages at 6h and 24h *p.i.* respectively, data not shown). While this feed forward regulation of TRIM14 mediated secondary expansion may explain the sustained levels of IFN in N24 infected cells, it does not account for the initial difference of IFN expression between the lineages.

Moreover, with the early IFN expression in macrophages, it was logical to assign a causative function to the initial events in the infection process. Two separate observations supported our hypothesis that intracellular localization early in infection would be primarily accountable for this differential IFN signaling by Mtb strains: 1) A huge spike in IFN response associated with BCG transfected as opposed to the negligible response in direct infection and 2) Absolute

requirement of even naked DNA to be deposited inside the cell (by transfection) as opposed to direct stimulation of cells with DNA.

Bacterial lysis by the phagosome-lysosome pathway has been implicated in several of the innate immune response pathways in phagocytes [33, 34]. Being an early event following infection, we monitored the intracellular trafficking of the different Mtb strains at different intervals post infection. Interestingly, we observed a direct correlation between phagosome-lysosome transit of Mtb strains and interferon inducing capacity; modern strains were observed at greater proportions in the acidified vesicles. While on the one hand only live bacteria were able to stimulate the macrophage type I IFN response, dead Mtb despite their well-documented higher rates of trafficking to acidified P-L compartments were unable to induce this response in macrophages hinting at the ability of modern Mtb's unique ability to utilize the host P-L pathway for active presentation of DNA (in contrast to dead bacteria that fail in this presentation) to the cytosolic signaling complex. On the other hand, Mtb of the L1 older lineage are reluctant P-L residents and thereby fail in their ability to efficiently present DNA to the IFN signaling complex.

Treatment of cells with a known acidification inhibitor- Baf A significantly reduced N24 mediated type I IFN induction in cells hinting on the importance of phagosomal acidification in type I IFN induction by Mtb. The contrasting increment in this response even in N73 infection due to enhanced acidification by LPS+IFNγ pretreatment further implies a novel adaptation by the modern lineage to harness the phagosome maturation pathway for modulating macrophage responses. In contrast, N73 transit to lysotracker positive vesicles at reduced levels and their possible retention within early endosomal compartments even in the later stages of infection (unpublished data) conforms to the well identified propensity of Mtb to modulate host cell phagosome maturation [35, 36, 37].

A dominant role for the Mtb sulfolipids have been demonstrated in modulation of the cellular phagosome maturation and acidification. Our results negate any putative role for this glycolipid in the intracellular bacterial localization and IFN response -1) differences in sulfolipid expression

between H37Ra and H37Rv is well established [38, 39], yet there was no discernable alteration of IFN expression between the two Mtb strains and 2) Expression of sulfolipid in N73 also does not augment IFN expression (data not shown).

Taken together, this study demonstrates two distinct methods of mycobacterial egress into the host trafficking network employed differently by strains to achieve optimal infection. Overall, we define a novel pathway of pro-inflammatory cytokine expression in Mtb induced macrophages involving the early innate type I IFN response and active modulation of the host cell oxysterol metabolism. Our results provide yet another example of the plasticity of Mtb as a human pathogen by evolving multiple facets of host response manipulation.

Material and Methods

Bacterial Strains and Growth Conditions—*M. tuberculosis* Erdman (Wt), a kind gift of Dr. Jeffrey Cox, USA, N0004, N0024 (Lineage 3), N0072, N0073 (Lineage 1) were isolated as part of the San Francisco collection of strains and kind gift of Dr. Sebastien Gagneux, Swiss TPH, Switzerland. All Mtb strains and BCG were grown in Middlebrook 7H9 broth (BD Biosciences, USA) containing 0.5% glycerol, 0.05% Tween80 and 4% acid-albumin-dextrose-catalase (ADC). Solid media (Middlebrook 7H10 agar, BD Biosciences, USA) was supplemented with 0.5% glycerol and 10% OADC (BD Biosciences, USA). Standard procedures were used for culturing *E. coli* strains in LB broth or agar (BD Biosciences, USA). Media was supplemented with kanamycin (20–50 μg /ml) or carbenicillin (100 μg/ml) when needed. The M6 promoter fragment was amplified as described earlier [40] and cloned upstream of GFP in the mycobacterial expression vector- pMV261. These plasmids were used to transform Mtb- N24 and N73 and recombinant clones were checked for expression of GFP. A list of primers used in this study is given in Table S1.

Macrophage culture and maintenance:

All the cell lines used were tested for mycoplasma contamination at regular intervals. THP1 cells were grown in HiglutaXL RPMI-1640 (Himedia laboratories, India) with 10% FBS and

differentiated by using PMA as described earlier [41]. For human monocyte derived macrophages (MDM), 20ml blood from individuals was collected in Heparin-EDTA tubes for isolation of PBMCs by density gradient separation using HiSep (Himedia laboratories, India) according to the recommended protocol. Following lysis of RBC, the PBMCs at a density of 1.25×10^6cells/ ml were differentiated to macrophages with RPMI containing 10% human sera (Himedia laboratories, India) and 50ng/ml GM-CSF (Invitrogen, USA) and the recommended concentration of Pen-Strep for 3 days. The cells were then washed and cultured in fresh media containing GM-CSF without any antibiotics for an additional 4 days and used for infection.

RAW264.7 (ECACC, UK), RAW-Lucia™ ISG and the knockout lines- RAW-Lucia™ ISG-KO-cGAS, STING, MAVS, RIG-1, MDA5, TRIF (Invivogen, France) were cultured according to standard conditions as per the manufacturer's recommendations. For infection with Mtb, cells were seeded at a density of 0.5×10^6/ml for 16-18h. For primary mouse macrophages, bone marrow cells were harvested from the hind limbs of C57Bl6 mice and differentiated into macrophages in 20% L- cell supernatant for 7 days as described earlier [42]. The differentiated macrophages were then harvested, counted and used for infection.

Preparation of Mtb fractions for stimulation of macrophages:

Mtb crude extracts were prepared from logarithmic liquid cultures with similar bacterial densities for the different strains. Cells were lysed with a mixture of 0.1 µm and 0.7 µm zirconia beads in PBS using a bead beater (Biospec India). The resultant lysates were cleared off the cell debris by high speed centrifugation and sterilized by filtering with a 0.2 µm filter and stored as aliquots at -20^{0}C. Before use, the protein content was determined and used to transfect THP1 dual cells using Lipofectamine LTX (Invitrogen, USA) reagent according to recommended protocol. Genomic DNA was isolated according to the manufacturer's recommendations (Nucleopore gDNA kit) and used for transfection. Enzymatic treatment of lysates was performed as: 1) Proteinase K- at 55^{0}C for 1h, 2) DNase, RNase at 37^{0}C for 1h and thermal denaturation at 96^{0}C for 30min.

Analysis of ESAT6 expression in Mtb:

Mtb cultures were grown to mid-logarithmic phase and the culture supernatant was collected by centrifugation at 3500rpm for 10 min. The supernatant was sterilized by filtration and proteins were precipitated with ice cold acetone and finally resuspended in water. Cell lysates were prepared by bead beating as described earlier and subjected to 15% SDS- PAGE. The proteins were transferred onto nitrocellulose and subjected to immunoblotting with anti ESAT6 monoclonal antibody HYB76-8.

Infection of macrophages with Mtb:

Mtb logarithmic cultures (0.6-0.8 O.D) were used for the preparation of single cells suspensions (SCS). Briefly, cells were harvested, washed and subjected to low speed centrifugation (800rpm for 5 min) to remove bacterial clumps. The SCS was then adjusted to the required MOI in fresh RPMI based on the absorbance measurements and used for infection.

At different time intervals, the cells/ RNA/ supernatants were harvested and used for analysis.

Intracellular compartmentalization of Mtb:

Lysotracker staining: Macrophages infected with fluorescent Mtb strains were used for intracellular bacterial localization by using Lysotracker – Red DND-99 (Invitrogen, USA) according to the recommended protocol. Briefly, at different time intervals, cells were washed to remove extracellular bacteria and incubated with 100nm Lysotracker Red in complete RPMI for 1h at 37^0C. The cells were washed to remove excess stain and fixed in 4% paraformaldehyde for 30 min, mounted on slides with Prolong diamond anti fade (Invitrogen, USA) and subjected to confocal microscopy. For estimating mitochondrial ROS by Mitosox staining, macrophages were washed thrice with PBS and stained with 5µM Mitosox (Invitrogen, USA) in HBSS for 30 min at 37^0C post infection. Cells were washed, fixed and subjected to high content microscopy in a IN Cell Analyzer 6000(GE healthcare life sciences, USA). Plasmid Mito-Dsred (kind gift from Dr. Sowmya Sinha Roy) was used to stably transfect THP1/ RAW 264.7 macrophages and used for analysis of mitochondrial architecture by epi fluorescence microscopy in the Leica TCS SP8 Confocal Microscope (Leica Microsystems, USA).

Analysis of gene expression by qRTPCR

Total RNA was isolated from macrophages suspended in Trizol by using the recommended protocol. cDNA was prepared from 1 µg of RNA by using the Verso cDNA synthesis kit and was used at a concentration of 10ng for expression analysis by using the DyNAmo Flash SYBR Green qPCR Kit (Thermo Fisher Scientific Inc., USA).

Transmission Electron Microscopy: Transmission electron microscopy (TEM) analysis of THP1 cells infected with Mycobacteria. THP1 cells were infected with mycobacteria at a MOI of 5 for 24h following which cells were collected and fixed in 2.5% gluteraldehyde and 4% paraformaldehyde, dehydrated in graded series of alcohol and embedded in Epon 812 resin. Ultrathin sections were cut and stained with uranyl acetate and lead citrate. TEM images were captured using Tecnai G2 20 twin (FEI) transmission electron microscope (FEI, Thermo Fisher Scientific Inc, USA).

Statistical Analysis

All experiments were performed in multiple biological replicates (N=2 or 3). Statistical analysis was done by using Student's t-test and corresponds to a *, **, *** for p-values<0.05, <0.01and <0.001, respectively.

Ethics Statement

The protocol for isolation of human blood PBMCs was approved by the Institutional Human ethics committee (Ref no: CSIR-IGIB/IHEC/2017-18 Dt. 08.02.2018). Blood was collected from people with their informed consent as per the Institutional guidelines**.**

Acknowledgements: The authors thank CSIR (VR-BSC0123), and DBT (GAP0096) funding agency for supporting the study. The authors thank Mr. Manish Kumar and CSIR- BSC0403 for the confocal microscopy facility. The Transmission Electron microscopy (TEM) and mass spectrometry facilities are duly acknowledged. The institute BSL3 facility project (STS0016) is duly acknowledged. The student fellowships from CSIR and DBT India are acknowledged. The support provided by Academy of Scientific and Innovative research (AcSIR) is duly acknowledged

Author Contributions: DS, PA, SG, VR were involved in conceptualizing and design of the work, the work was performed by PA and DS. VR, PA and DS were involved in the manuscript preparation and proof reading.

Table S1: A List of primers used in the study

IL-6 FP	ACAAGAAAGACAAAGCCAG
IL-6 RP	TGTGACTCCAGCTTATCTG
Hmgcs1 FP	TGGCACAGTACTCACCTC
Hmgcs1 RP	CCTTCATCCAAACTGTGG
HMGCR FP	CTTGTGGAATGCCTTGTGATTG
HMGCR RP	AGCCGAAGCAGCACATGAT
Idi1 FP	TGGGAATACCCTTGGAAGAG
Idi1 RP	CCCCAGATACCATCAGATTG
Fdft1 FP	CCACCCGGAGGAGTTCTAT
Fdft1 RP	AAGCTGCGACTGGTCTGATT
Cyp51 FP	CTTGCTTTCCACGCTGCTCATC
Cyp51 RP	GCATGGCCAAGGAATGGAATTGG
Sc4mol FP	AGAATACGCACATCCCTTGG
Sc4mol RP	GCGGGTTGAGAGGAATATCA
Nsdhl FP	AAACCTGGTGGACTTCACCTTCGT
Nsdhl RP	AGGAACGTCCAGAAAGGGATTGGT
Dhcr24 FP	AGTCATCGTCCCACAAGTAT
Dhcr24 RP	CTCTACGTCGTCCGTCAT
Ch25h FP	GACCTTCTTCGACGTGCTGA
Ch25h RP	CCACCGACAGCCAGATGTTA
Gapdh FP	TTCACCACCATGGAGAAGGC
Gapdh RP	GGCATGGACTGTGGTCATGA
hIP10 FP	TCCACGTGTTGAGATCATTGC
hIP10 RP	GGCCTTCGATTCTGGATTCAG
hIFIT2 FP	CGAACAGCTGAGAATTGCAC
hIFIT2 RP	CAAGTTCCAGGTGAAATGGC
hIFN-β FP	AGCAGTTCCAGAAGGAGGAC
hIFN-β RP	TGATAGACATTAGCCAGGAGGTT
hGapdh FP	GAAGGTGAAGGTCGGAGTC
hGapdh RP	GAAGATGGTGATGGGATTTC

References

575 1. Stanley SA, Johndrow JE, Manzanillo P, Cox JS. The Type I IFN response to infection with
576 Mycobacterium tuberculosis requires ESX-1-mediated secretion and contributes to
577 pathogenesis. *J Immunol* **178**, 3143-3152 (2007).

578
579 2. Wassermann R*, et al.* Mycobacterium tuberculosis Differentially Activates cGAS- and
580 Inflammasome-Dependent Intracellular Immune Responses through ESX-1. *Cell Host Microbe*
581 **17**, 799-810 (2015).

582
583 3. McNab FW*, et al.* Type I IFN induces IL-10 production in an IL-27-independent manner and
584 blocks responsiveness to IFN-gamma for production of IL-12 and bacterial killing in
585 Mycobacterium tuberculosis-infected macrophages. *J Immunol* **193**, 3600-3612 (2014).

586
587 4. Wiens KE, Ernst JD. The Mechanism for Type I Interferon Induction by Mycobacterium
588 tuberculosis is Bacterial Strain-Dependent. *PLoS Pathog* **12**, e1005809 (2016).

589
590 5. Collins AC*, et al.* Cyclic GMP-AMP Synthase Is an Innate Immune DNA Sensor for Mycobacterium
591 tuberculosis. *Cell Host Microbe* **17**, 820-828 (2015).

592
593 6. Pandey AK*, et al.* NOD2, RIP2 and IRF5 play a critical role in the type I interferon response to
594 Mycobacterium tuberculosis. *PLoS Pathog* **5**, e1000500 (2009).

595
596 7. Redford PS*, et al.* Influenza A virus impairs control of Mycobacterium tuberculosis coinfection
597 through a type I interferon receptor-dependent pathway. *J Infect Dis* **209**, 270-274 (2014).

598
599 8. Weiss G, Schaible UE. Macrophage defense mechanisms against intracellular bacteria. *Immunol*
600 *Rev* **264**, 182-203 (2015).

601
602 9. Teles RM*, et al.* Type I interferon suppresses type II interferon-triggered human anti-
603 mycobacterial responses. *Science* **339**, 1448-1453 (2013).

604
605 10. Manca C*, et al.* Hypervirulent M. tuberculosis W/Beijing strains upregulate type I IFNs and
606 increase expression of negative regulators of the Jak-Stat pathway. *J Interferon Cytokine Res* **25**,
607 694-701 (2005).

608
609 11. Liu SY*, et al.* Interferon-inducible cholesterol-25-hydroxylase broadly inhibits viral entry by
610 production of 25-hydroxycholesterol. *Immunity* **38**, 92-105 (2013).

611
612 12. Blanc M*, et al.* The transcription factor STAT-1 couples macrophage synthesis of 25-
613 hydroxycholesterol to the interferon antiviral response. *Immunity* **38**, 106-118 (2013).

614
615 13. Gold ES*, et al.* 25-Hydroxycholesterol acts as an amplifier of inflammatory signaling. *Proc Natl*
616 *Acad Sci U S A* **111**, 10666-10671 (2014).

617
618 14. Diczfalusy U, *et al.* Marked upregulation of cholesterol 25-hydroxylase expression by
619 lipopolysaccharide. *J Lipid Res* **50**, 2258-2264 (2009).

620
621 15. Bah SY, Dickinson P, Forster T, Kampmann B, Ghazal P. Immune oxysterols: Role in
622 mycobacterial infection and inflammation. *J Steroid Biochem Mol Biol* **169**, 152-163 (2017).

623
624 16. Liu CH, Liu H, Ge B. Innate immunity in tuberculosis: host defense vs pathogen evasion. *Cell Mol*
625 *Immunol*, (2017).

626
627 17. Xu G, Wang J, Gao GF, Liu CH. Insights into battles between Mycobacterium tuberculosis and
628 macrophages. *Protein Cell* **5**, 728-736 (2014).

629
630 18. Petit-Jentreau L, Tailleux L, Coombes JL. Purinergic Signaling: A Common Path in the
631 Macrophage Response against Mycobacterium tuberculosis and Toxoplasma gondii. *Front Cell*
632 *Infect Microbiol* **7**, 347 (2017).

633
634 19. Dorhoi A, *et al.* Type I IFN signaling triggers immunopathology in tuberculosis-susceptible mice
635 by modulating lung phagocyte dynamics. *Eur J Immunol* **44**, 2380-2393 (2014).

636
637 20. Sun J, Wang X, Lau A, Liao TY, Bucci C, Hmama Z. Mycobacterial nucleoside diphosphate kinase
638 blocks phagosome maturation in murine RAW 264.7 macrophages. *PLoS One* **5**, e8769 (2010).

639
640 21. Vergne I, Fratti RA, Hill PJ, Chua J, Belisle J, Deretic V. Mycobacterium tuberculosis phagosome
641 maturation arrest: mycobacterial phosphatidylinositol analog phosphatidylinositol mannoside
642 stimulates early endosomal fusion. *Mol Biol Cell* **15**, 751-760 (2004).

643
644 22. Martin FJ, *et al.* Staphylococcus aureus activates type I IFN signaling in mice and humans
645 through the Xr repeated sequences of protein A. *J Clin Invest* **119**, 1931-1939 (2009).

646
647 23. Castiglia V, *et al.* Type I Interferon Signaling Prevents IL-1beta-Driven Lethal Systemic
648 Hyperinflammation during Invasive Bacterial Infection of Soft Tissue. *Cell Host Microbe* **19**, 375-
649 387 (2016).

650
651 24. Watanabe T, *et al.* NOD1 contributes to mouse host defense against Helicobacter pylori via
652 induction of type I IFN and activation of the ISGF3 signaling pathway. *J Clin Invest* **120**, 1645-
653 1662 (2010).

654
655 25. Hansen K, *et al.* Listeria monocytogenes induces IFNbeta expression through an IFI16-, cGAS-
656 and STING-dependent pathway. *Embo J* **33**, 1654-1666 (2014).

657

658 26. Abdullah Z*, et al.* RIG-I detects infection with live Listeria by sensing secreted bacterial nucleic
659 acids. *Embo J* **31**, 4153-4164 (2012).

660
661 27. Boxx GM, Cheng G. The Roles of Type I Interferon in Bacterial Infection. *Cell Host Microbe* **19**,
662 760-769 (2016).

663
664 28. Pinto SM*, et al.* Integrated Multi-Omic Analysis of Mycobacterium tuberculosis H37Ra Redefines
665 Virulence Attributes. *Front Microbiol* **9**, 1314 (2018).

666
667 29. Wilkins C, Gale M, Jr. Sterol-izing innate immunity. *Immunity* **38**, 3-5 (2013).

668
669 30. Zimmermann M*, et al.* Integration of Metabolomics and Transcriptomics Reveals a Complex Diet
670 of Mycobacterium tuberculosis during Early Macrophage Infection. *mSystems* **2**, (2017).

671
672 31. Wang X*, et al.* STING Requires the Adaptor TRIF to Trigger Innate Immune Responses to
673 Microbial Infection. *Cell Host Microbe* **20**, 329-341 (2016).

674
675 32. Chen M*, et al.* TRIM14 Inhibits cGAS Degradation Mediated by Selective Autophagy Receptor
676 p62 to Promote Innate Immune Responses. *Mol Cell* **64**, 105-119 (2016).

677
678 33. Herskovits AA, Auerbuch V, Portnoy DA. Bacterial ligands generated in a phagosome are targets
679 of the cytosolic innate immune system. *PLoS Pathog* **3**, e51 (2007).

680
681 34. Ip WK*, et al.* Phagocytosis and phagosome acidification are required for pathogen processing
682 and MyD88-dependent responses to Staphylococcus aureus. *J Immunol* **184**, 7071-7081 (2010).

683
684 35. Kelley VA, Schorey JS. Mycobacterium's arrest of phagosome maturation in macrophages
685 requires Rab5 activity and accessibility to iron. *Mol Biol Cell* **14**, 3366-3377 (2003).

686
687 36. Vergne I, Chua J, Lee HH, Lucas M, Belisle J, Deretic V. Mechanism of phagolysosome biogenesis
688 block by viable Mycobacterium tuberculosis. *Proc Natl Acad Sci U S A* **102**, 4033-4038 (2005).

689
690 37. Via LE, Deretic D, Ulmer RJ, Hibler NS, Huber LA, Deretic V. Arrest of mycobacterial phagosome
691 maturation is caused by a block in vesicle fusion between stages controlled by rab5 and rab7. *J*
692 *Biol Chem* **272**, 13326-13331 (1997).

693
694 38. Gonzalo Asensio J*, et al.* The virulence-associated two-component PhoP-PhoR system controls
695 the biosynthesis of polyketide-derived lipids in Mycobacterium tuberculosis. *J Biol Chem* **281**,
696 1313-1316 (2006).

697

39. Walters SB, Dubnau E, Kolesnikova I, Laval F, Daffe M, Smith I. The Mycobacterium tuberculosis PhoPR two-component system regulates genes essential for virulence and complex lipid biosynthesis. *Mol Microbiol* **60**, 312-330 (2006).

40. Arumugam P, Shankaran D, Bothra A, Gandotra S, Rao V. The MmpS6-MmpL6 Operon Is an Oxidative Stress Response System Providing Selective Advantage to Mycobacterium tuberculosis in Stress. *J Infect Dis* **219**, 459-469 (2019).

41. Bothra A*, et al.* Phospholipid homeostasis, membrane tenacity and survival of Mtb in lipid rich conditions is determined by MmpL11 function. *Sci Rep* **8**, 8317 (2018).

42. Rao V, Fujiwara N, Porcelli SA, Glickman MS. Mycobacterium tuberculosis controls host innate immune activation through cyclopropane modification of a glycolipid effector molecule. *J Exp Med* **201**, 535-543 (2005).

Supplementary figures:

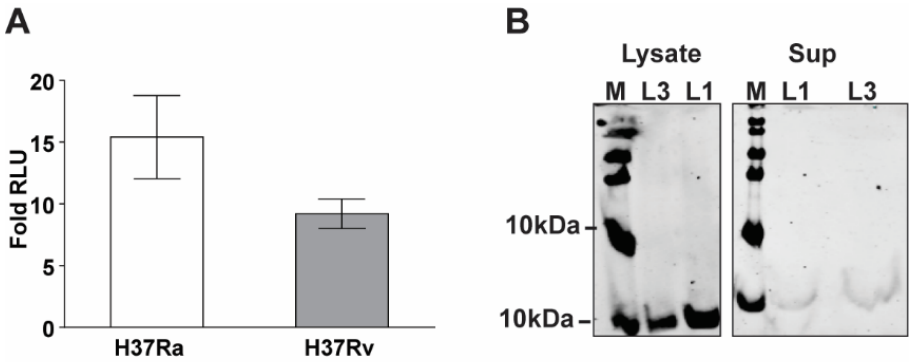

Fig.S1

A) Relative luminescence in THP1 macrophages infected with H37Ra and Rv at 24h post infection. ESAT6 expression in culture supernatant and lysates of Mtb N24 and N73.

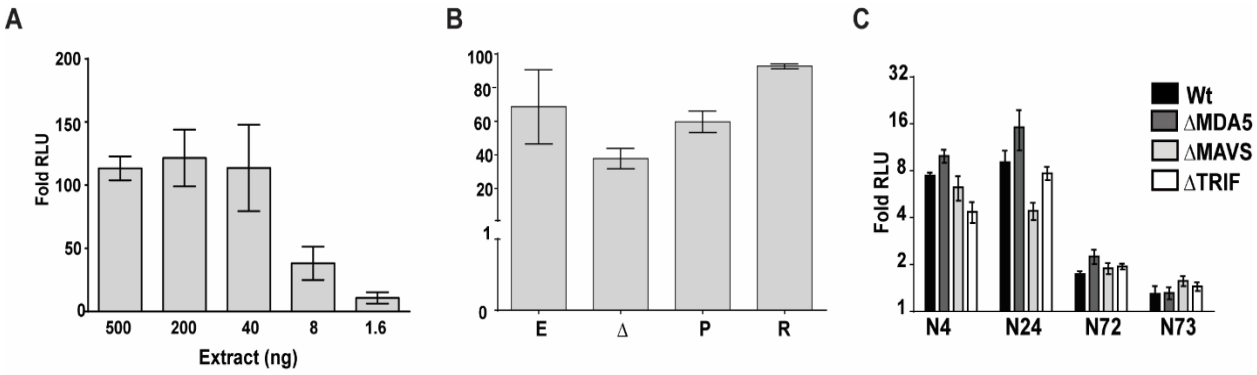

Fig.S2

A) Dose dependent IRF induction by Mtb crude extracts at 6h.
B) IRF induction by enzymatically digested 500ng of Mtb crude extracts at 6h.
C) Relative luminescence in RAW WT and KO macrophages infected with L3 and L1 Mtb at 24h post infection.

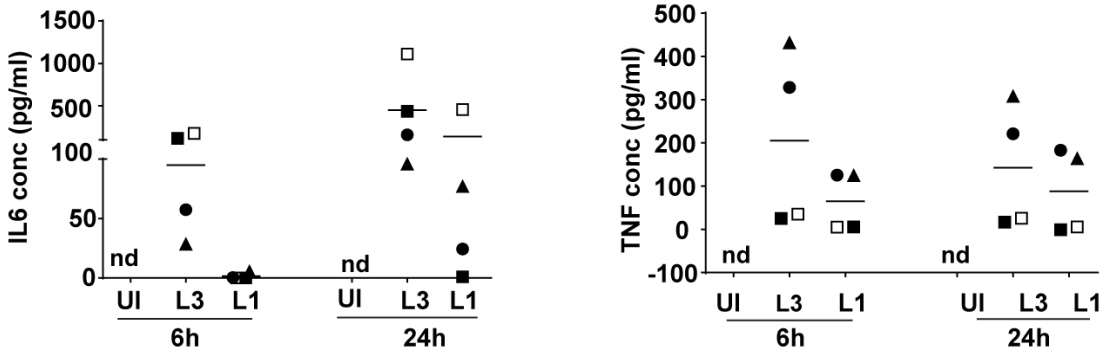

Fig. S3

IL6 and TNF secretion from human MDMs from four individuals left uninfected (UI) or following infection with L3 or L1 strains at 6h and 24h p.i. Values represent mean cytokine concentration in pg/ml in the culture supernatant of triplicate wells for each individual.

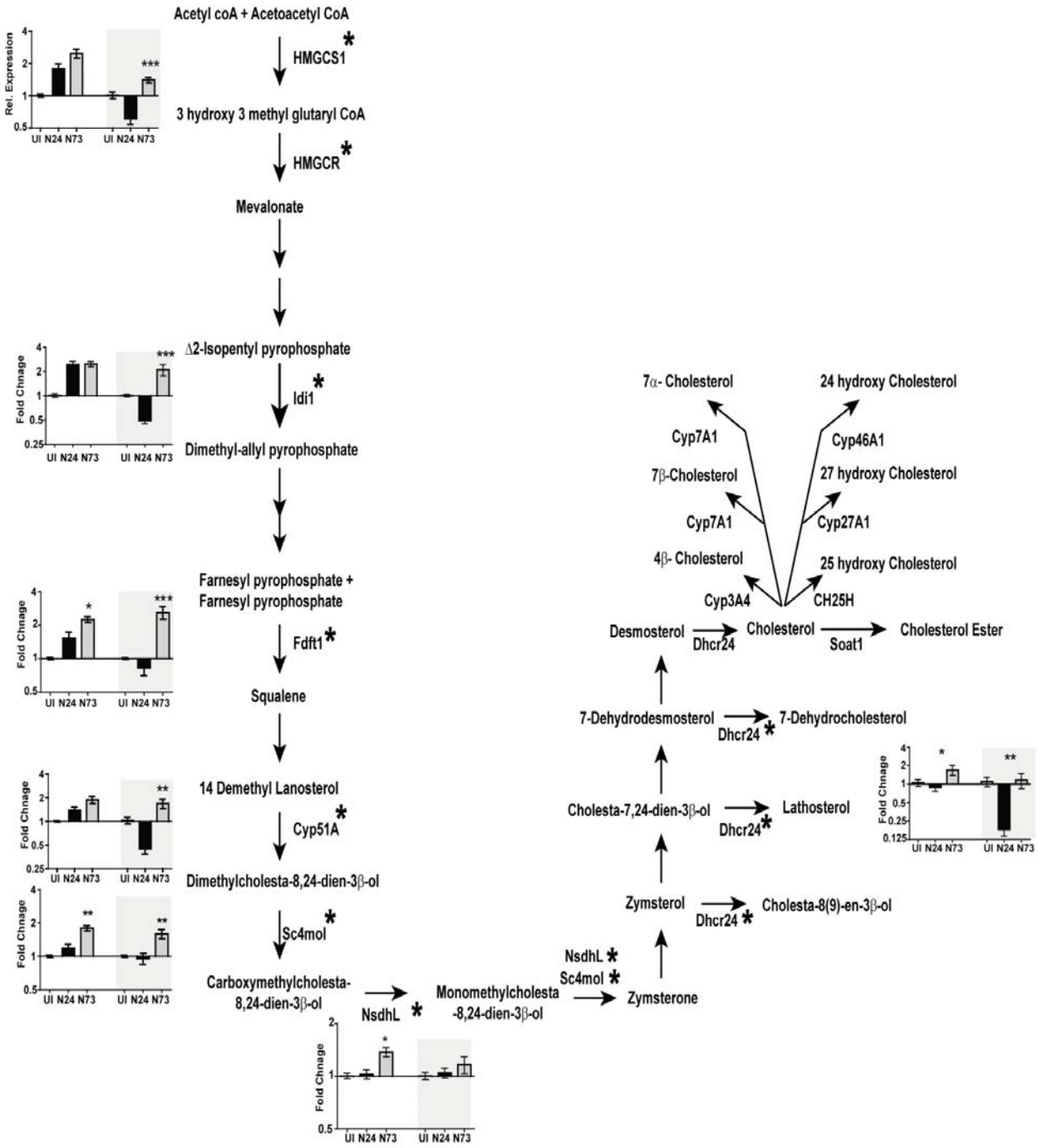

Fig.S4

Expression of genes involved in cholesterol biosynthesis in macrophages infected with N24 or N73 at 6h and 24h (shaded) estimated by qRTPCR.

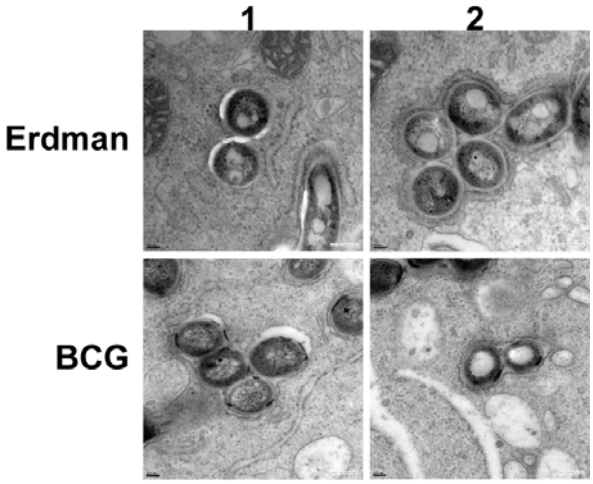

Fig.S5

Electron micrographs of THP1 macrophages infected with Mtb Erdman and BCG at 24h p.i.

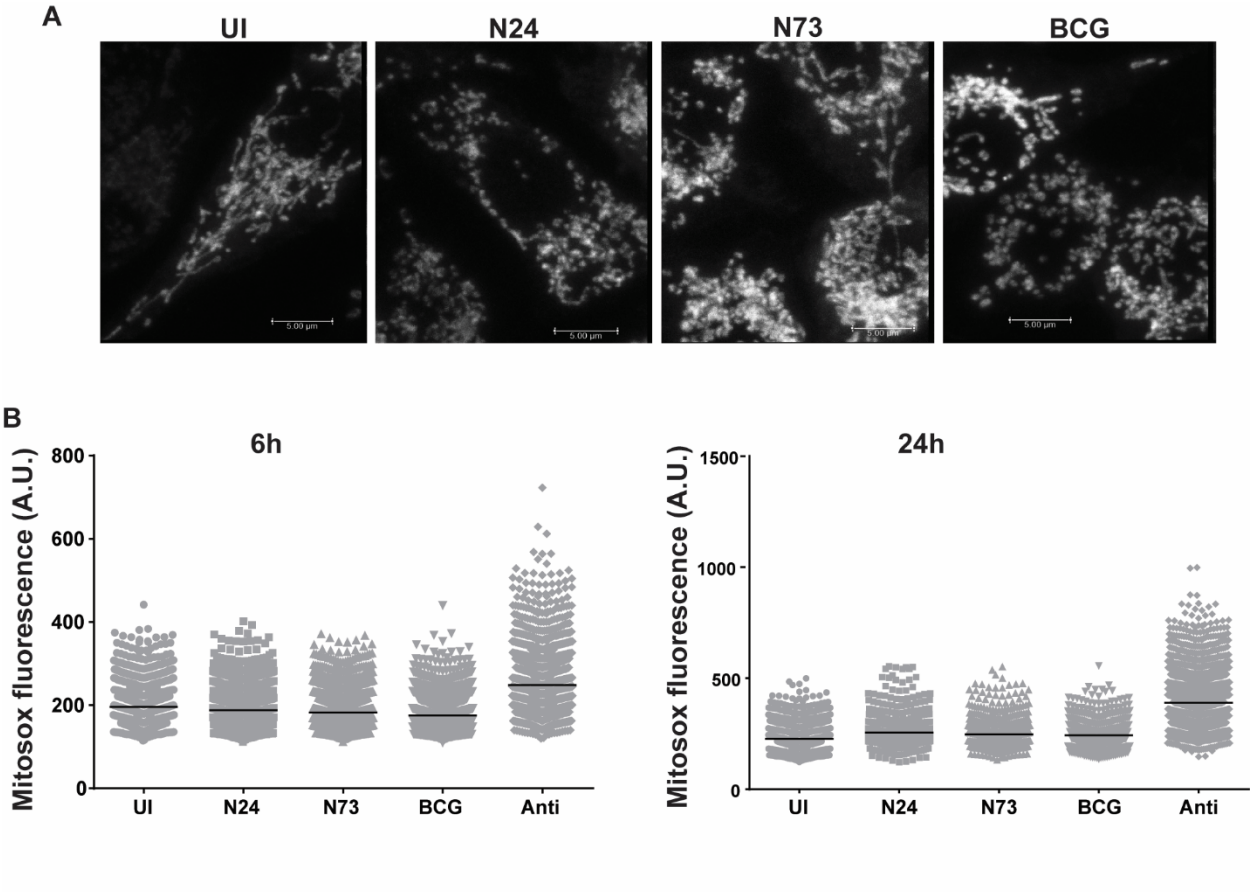

Fig.S6

A) Mitochondrial architecture at 24h post infection with mycobacterial strains. Uninfected macrophages (UI) was used as a control.

B) Quantitation of mitochondrial ROS by mitosox staining following infection with mycobacteria or treatment of Antimycin A (+ control) at 6h and 24h.